



ISSN: 1813-162X (Print); 2312-7589 (Online)

Tikrit Journal of Engineering Sciences

available online at: <http://www.tj-es.com>TJES
Tikrit Journal of
Engineering Sciences

Investigating The Behavior of Steel-Concrete Composite Arch Beam with Different Types of Shear Connectors

Yousif Th. Alhassankoo ^a, Suhaib Y. Al-Darzi ^a, Kaythar A. Ibrahim ^{b*}^a Civil Engineering Department, College of Engineering, University of Mosul, Mosul, Iraq.^b Environmental Engineering Department, College of Engineering, University of Mosul, Mosul, Iraq.**Keywords:**

Arch beam; Steel I-section-concrete composite arch members; Steel plate-concrete composite arch members; Shear connector; Push-out test.

Highlights:

- Two types of steel-concrete composite arch beams were used.
- Experimental test was carried out by adopting four types of shear connectors.
- Push-out test for the four connector types was conducted.

ARTICLE INFO**Article history:**

Received	26 May	2023
Received in revised form	19 Aug.	2023
Accepted	06 Jan.	2024
Final Proofreading	02 Aug.	2024
Available online	05 Sep.	2024

© THIS IS AN OPEN ACCESS ARTICLE UNDER THE CC BY LICENSE. <http://creativecommons.org/licenses/by/4.0/>



Citation: Alhassankoo YT, Al-Darzi SY, Ibrahim KA. Investigating the Behavior of Steel-Concrete Composite Arch Beam with Different Types of Shear Connectors. *Tikrit Journal of Engineering Sciences* 2024; 31(3): 233-245.

<http://doi.org/10.25130/tjes.31.3.22>

***Corresponding author:****Kaythar A. Ibrahim**

Environmental Engineering Department, College of Engineering, University of Mosul, Mosul, Iraq.

Abstract: Composite steel-concrete arch beams are used in civil engineering. The effect of the shear connector type on the behavior of this type of beam was to act as the first parameter in this study. The test used four types of shear connectors: stud, angle, perfobond, and rebar. The second parameter involved two composite section types: steel I-section-concrete composite arch members (SICM) and steel plate-concrete composite arch members (SPCM). A total of eight samples were prepared in two groups. The first used the SICM and four connector types to get four samples: stud (SI), angle (AI), perfobond (PI), and rebar connector (RI). The second used the SPCM and the same connectors to get SP, AP, PP, and RP, respectively. All samples were tested under one concentrated load at the top of the arch with fixed supports at both ends. A push-out test for the four connector types was also conducted. For all samples, the SICM showed a higher ultimate load than the SPCM. For the SICM, the samples had close values for the maximum load, with the PI sample having the highest. For the SPCM, the SP sample recorded maximum load and deflection. The failure shear crack in all samples appeared at the top of the concrete in the arch beam crown and extended to the bottom, making an angle between 30-45 degrees. It was concluded that the main reason for the failure was the high vertical slips for the top connectors; therefore, the connectors should be designed to resist high tensile forces, and the transverse reinforcing bar should be carefully placed and sized.

سلوك الخضوع للعتبات الفولاذية نتيجة لشكل مسار تثبيت السلك مسبق المجهد

يوسف ذاك حازم¹، صهيب يحيى قاسم¹، قيثار عبدالوهاب إبراهيم²

¹ قسم الهندسة المدنية / كلية الهندسة / جامعة الموصل / الموصل - العراق.

² قسم هندسة البيئة / كلية الهندسة / جامعة الموصل / الموصل - العراق.

الخلاصة

تستخدم الاعتاب المقوسة المركبة حديد-كونكريت في الهندسة المدنية لمقاومة الاحمال العالية ان تأثير انواع روابط القص على سلوك هذا النوع من الاعتاب كان المتغير الاول لهذه الدراسة حيث تم الفحص العملي باعتماد أربعة أنواع من روابط القص: رباط قص مسمار (Stud)، رباط قص زاوية (Angle)، رباط قص بيرفوبوند (Perfobond)، و رباط قص قضيب تسليح (Rebar). تضمن المتغير الثاني للبحث استخدام نوعين من المقاطع المركبة: عتب مقوس مركب باستخدام مقطع حديد (I) - خرسانة (SICM) و عتب مقوس مركب باستخدام ألواح حديد-خرسانة (SPCM). تم تحضير ثمان نماذج في مجموعتين، الأولى استخدمت SICM وروابط القص الأربعة للحصول على أربع نماذج: مسمار (SI)، زاوية (AI)، بيرفو بوند (PI)، قضيب تسليح (RI). المجموعة الثانية استخدمت المقطع SPCM ونفس روابط القص للحصول على SP و AP و PP و RP على التوالي. تم فحص جميع النماذج تحت تأثير حمولة واحدة مركزة في الجزء العلوي من القوس مع مساند موثقة في كلا الطرفين. تم أيضاً إجراء فحص الدفع لروابط القص الأربعة. اظهرت النتائج ان الحمل الاقصى لجميع النماذج التي استخدمت المقطع SICM اكبر من تلك التي استخدمت المقطع SPCM. تم تسجيل قيم مقاربة للحمل الاقصى لنماذج SICM و اعلى قيمة سجلت للنموذج PI. بالنسبة لنماذج SPCM سجل النموذج SP اعلى حمل اقصى واعلى هطول. ظهر صدع فشل القص في جميع النماذج في الجزء العلوي من خرسانة العتب المقوس وامتد إلى الجناح السفلي للقوس بزواوية تتراوح بين 30-45 درجة. تم التوصل الى ان السبب الرئيسي للفشل يرجع إلى الانزلاق الرأسي لروابط القص العلوية، لذلك يتوجب تصميم روابط القص لتحمل قوى الشد بشكل اساسي واختيار عدد قضبان التسليح العرضية وقطرها بعناية.

الكلمات الدالة: عناصر قوسية مركبة من الصلب على شكل حرف I-خرسانة، عناصر قوسية مركبة من ألواح فولاذية-خرسانة، موصل القص، اختبار الدفع للخارج.

1. INTRODUCTION

Steel-concrete composite beams are frequently used in civil engineering because they combine the mechanical advantages of the primary constituent materials, such as steel and concrete. Concrete is distinguished from structural steel by its high stiffness and significant compressive strength, whereas structural steel is distinguished by its high tensile strength and ductility [1-3]. Steel-concrete composite is the most prevalent type of composite material used in construction. However, there are many other types of composites, such as steel-timber, timber-concrete, plastic-concrete, CFRP, and others [4-6]. Although new shapes of composite members have been suggested [7,8], steel beams and reinforced concrete slabs were utilized together for many years without regard for their composite properties. In recent decades, however, it has been demonstrated that connecting the two so that they resist loads as a unit produced a significant strengthening effect. Steel beams and concrete slabs can frequently support 33 to 50 percent or more load than when acting in a non-composite manner [9]. Hence, less steel is used for the same loads and spans. Composite sections have the greatest stiffness and, therefore, the least deflections than non-composite sections. Moreover, the composite structure allows for overall shallower floor depths [10]. The fact that lesser floor depths permit shorter building heights, resulting in lower costs for walls, plumbing, wiring, ducts, elevators, and foundations, is particularly significant for tall buildings. Because fireproofing material is applied to smaller and shallower steel shapes, the fireproofing expenses decline, which is a significant advantage of reduced beam depths [11]. Using vaults and arches to cross horizontal areas dates back several thousand years. The earliest arches were discovered in Mesopotamian underground tombs

constructed in approximately 3000 BC. [12]. In addition to the Sumerians, the Egyptians and Greeks were also skilled at building vaults and arches [13]. An arch is a curving girder with convexity in the upward direction and is supported at its endpoints. Enhancing the load-carrying capacity is the major goal of the arch, which may be accomplished by the stiffening behavior brought on by the membrane action. By utilizing materials with effective compressive strength, such as concrete, structural engineers could accomplish large spans in buildings' roofing and bridge decking [14,15]. At the steel-concrete interface, shear connectors play a crucial role. Conventional shear connectors are often constructed of steel and come in the shapes of studs, steel elements, bent-up bars, and perforated bond leiste (PBL) shear connectors [16,17]. Shear connections are capable of withstanding the horizontal force acting on the interface and the lift displacement that occurs when steel and concrete are joined together. Although different materials have different elastic moduli, steel and concrete can work together using shear connectors [18]. Fan and Zhou [18] studied the Perfobond Hoop (PBH), a new proposed shear connector depending on the Perfobond Leisten (PBL) connectors, with the main objective of using steel box-concrete composite sections for composite arch members. The steel box-concrete composite sections had better mechanical properties through experiments and research and were, therefore, suitable for widespread use in bridge engineering. Ali and Kadhum [19] investigated the behavior and performance of hollow, curved reinforced concrete beams with and without openings in un-strengthened and strengthened conditions. The horizontal displacement, ultimate deflection of the roller end, and the maximum load-carrying capacity were experimentally determined and compared with the control

beam (with no opening). The failure mode of all the specimens was compared with the control beam to investigate the opening's shape and location impact on each specimen's overall behavior and check the opening strengthening method impact proposed by Mansur [20]. Zhou et al. [21] proposed the geological characteristics and environmental requirements of the Zaodu Bridge, a vertical rotating steel box-concrete composite arch bridge, based on a comprehensive analysis of existing concrete arch bridges' structure and construction technology. Steel and concrete are used in different regions according to the mechanical requirements of the structure, demonstrating the material superiority of both materials. Ali and Hamza [22] used the finite element method to evaluate the behavior and performance of reinforced concrete arches with and without apertures, un-strengthened and strengthened (externally by CFRP laminates or internally by steel reinforcement) and compare the findings to experimental study. The following variables were considered in that study: curvature forces, the opening location through the arch's profile, and the type of strengthening. The ANSYS computer program was used throughout this study. The finite element and experimental results showed good agreement with regard to the load-deflection response and mode of failure, where cracking and ultimate loads had average differences of about 5.83% and 3.92%, respectively. Jayanthi and Umrani [23] studied shear connectors for steel-concrete composite construction to transmit longitudinal shear, prevent the separation of steel and concrete slabs, and improve the structural effectiveness of the entire system. Push-out tests under monotonic loading circumstances were used to assess the performances of several shear connector types in steel-concrete composite specimens. Ibrahim et al. [24] examined the flexural behavior of composite beams made of steel tubes with square, rectangular, and hexagonal sections using the same kind of shear connector, i.e., headed stud, angle, or perfbond. Lu et al. [25] conducted experimental and analytical modal studies of the 110-meter-long Shizhi River Bridge, a special-shaped composite arch bridge made of concrete-filled steel tubes. Using a three-dimensional finite element model (FEM) and analytical modal analysis, the bridge's static behavior, natural frequencies, and mode shapes were found. Under static loads and forced excitations, studies in static, stable, and dynamic fields were performed. The experimental methods comprised a static investigation under five loading conditions. It was discovered that the results from the finite element model and the experimental set were

strongly agreed. Nimnim and Fakhri [26] conducted experimental research to study the flexural behavior and ultimate strength of concrete arched slabs. It was found that the effects of raising f_c from 30 MPa to 65 MPa ranged from an increasing effect of 15% to 25% on the ultimate load to a reducing effect of 55% to 73% on the ultimate deflection. Also, increasing the thickness by 42% tended to lower the ultimate deflection, which ranged from 17% to 64%, while increasing the ultimate load, which ranged from 6% to 17%. The research and specifications for steel-concrete composite arch members showed a rather poor level of behavior and capacity. There are several practical studies on this type of composite steel member. However, the primary distinction is that the member used for this research was curved rather than straight. Two composite sections were used: Steel I-section-concrete composite arch members (SICM) and steel plate-concrete composite arch members (SPCM). The SICM is commonly used in construction. While the SPCM was evaluated in this study. Four connectors were adopted for investigation: a stud, angle, perfbond, and rebar connector.

2. MATERIAL PROPERTIES

Local materials were used for casting all concrete samples. Sand and rounded gravel from the Badush area were used, while the cement was chosen from the Badush factory. The chemical and physical properties were tested in the University of Mosul lab. The results are shown in Table 1. The sieve analysis of sand and rounded coarse aggregate is shown in Tables 2 and 3. All values lie within the limits of Iraqi standards IQS:45/2010 [27], as shown in Tables 2 and 3. The specific gravity of fine and coarse aggregate (ASTM C128, C127) [28,29] was 2.7 and 2.6, respectively. The fineness modulus for sand (ASTM C 136) [30] was 2.8. 8 mm diameter steel bars were used as a reinforcement in all samples. The properties of steel reinforcement are tabulated in Table 4. The test was conducted according to ASTM A615/A615M-20 [31], as shown in Fig. 1. The concrete mix was designed to achieve the desired 32 MPa compressive strength after 28 days. ACI Standard Practice ACI 211.1-91 was used to determine the mixed concrete proportions [32]. Before casting concrete specimens, a mix was made, tested, and cast. The resulting mixing ratio of cement, sand, and gravel was 1:2:2.18, and the W/C was 0.44. ASTM C143/C143M-12 was used to measure the slump [33], i.e., 160 mm. The cylinders were tested according to ASTM 39 [34] and listed in Table 5. All tests were conducted in the College of Engineering laboratories at the University of Mosul.

Table 1 Physical Properties and Chemical Component of the Cement.

Physical Properties	Units	Value	Limitations
Standard Consistency w/c	-	0.25	----
Initial setting	Minutes	150	≥ 45
Final setting	Minutes	315	≤ 600
Compressive strength (3 days)	MPa	21.1	≥ 15
Compressive strength (7 days)	MPa	30	≥ 23
Fineness (sieve no. 170)	%	4.6	≤ 10
Chemical Components	Units	Value	Limitations
SiO ₂	%	20.6	-
Al ₂ O ₃	%	4.9	-
Fe ₂ O ₃	%	2.6	-
CaO	%	64.64	-
MgO	%	3.32	≤ 5
SO ₃	%	1.58	≤ 2.5
Free Lime	%	2.9	-
Loss on ignition	%	2.61	≤ 4
Insoluble residue	%	0.4	≤ 1.5
Total	%	100.24	-
C ₃ S	%	53.64	-
C ₂ S	%	18.59	-
C ₃ A	%	8.58	-
C ₄ AF	%	7.92	-
L.S.F.	%	97.37	-
Solid Solution	%	14.71	-

Table 2 Sieve Analysis of Sand.

Sieve size (mm)	Passing %	Passing% Zone2 Limits (IQS:45/2010)
4.75	100	90-100
2.36	84.2	75-100
1.18	64	55-90
0.6	45.6	35-59
0.3	21.2	8-30
0.15	4.8	0-10

Table 3 Sieve Analysis of Course Aggregates.

Sieve size (mm)	Passing %	Passing% Limits (IQS:45/2010)
20	100	100
14	95	90-100
10	65	50-85
5	0	0-10

Table 4 Properties of Steel Reinforcement.

Sample No.	Yield Stress (N/mm ²)	Ultimate Stress (N/mm ²)	Elongation
1	514	627	16.6%
2	525	630	19.3%

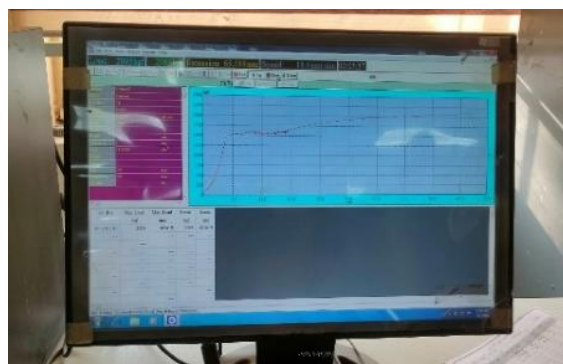


Fig. 1 Steel Reinforcement Test by Universal Testing Machine.

Table 5 Results of Cylinder Compressive Strength.

Cylinder Age	First sample	Second sample	Third sample	Average
7 Days	21.4	21.5	22	21.6
28 Days	31.9	34	33.1	33

3. EXPERIMENTAL WORK

This study used four types of connectors to experimentally investigate the behavior of Steel I-section-concrete composite arch members (SICM) and steel plate-concrete composite arch members (SPCM). Both ends of the arches were fixed. The first group included four samples of SICM connected with a concrete deck with the dimensions and details shown in Figs. 2 and 3. The flange and web thicknesses were 6 mm and 4 mm, respectively.

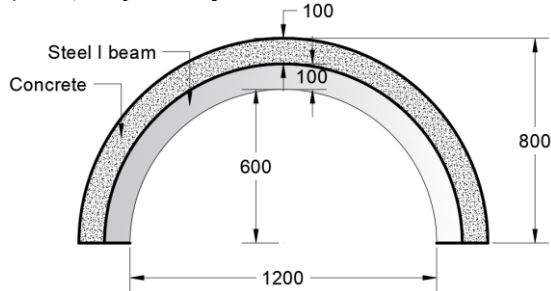


Fig. 2 Geometry for I SICM.

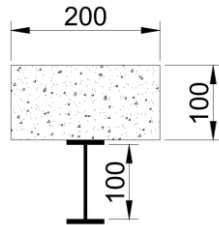


Fig. 3 Section for SICM.

The second group includes four samples prepared for investigating SPCM, as shown in Figs. 4 and 5. The steel plate was 8 mm thick.

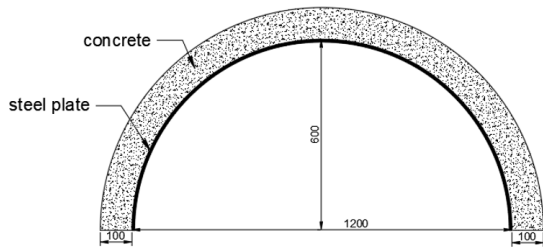


Fig. 4 Geometry for SPCM.

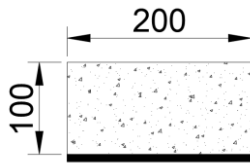


Fig. 5 Section for SPCM.

The steel I beams and plates were tested and found to meet the requirements of ASTM A36 [35]. The following four types of connectors were used:

- 1) Steel studs.
- 2) Steel Angle connector.
- 3) Steel Perfobond connector.
- 4) Steel Rebar connector.

The details of the connectors are shown in Fig. 6.

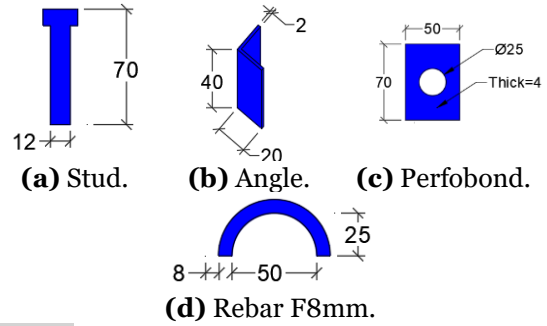


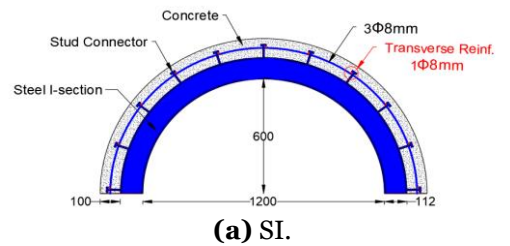
Fig. 6 Connectors Types (dimensions in mm).

The work extended to find the behavior and strength of shear connectors through push-out tests for each type of connector used in the samples. Table 6 lists details of the samples used in this study.

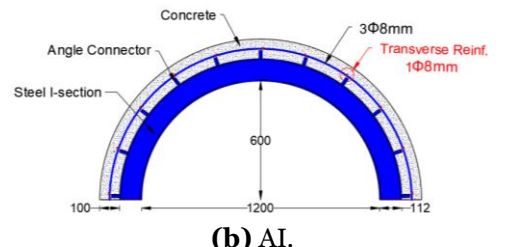
Table 6 Details of Arch Beams.

ID	Composite Arch Member Type	Connector Type	Sample Code
1	SICM	Stud	SI
2	SICM	Angle	AI
3	SICM	Perfobond	PI
4	SICM	Rebar	RI
5	SPCM	Stud	SP
6	SPCM	Angle	AP
7	SPCM	Perfobond	PP
8	SPCM	Rebar	RP

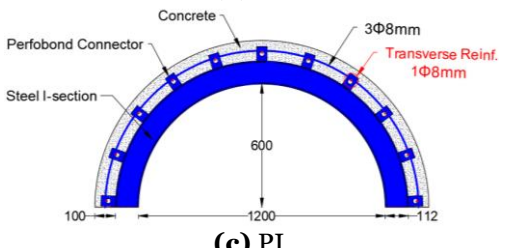
The Details of the samples can be shown in Figs. 7 and 8.



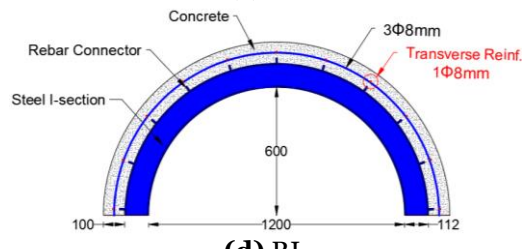
(a) SI.



(b) AI.



(c) PI.



(d) RI.

Fig. 7 SICM Samples.

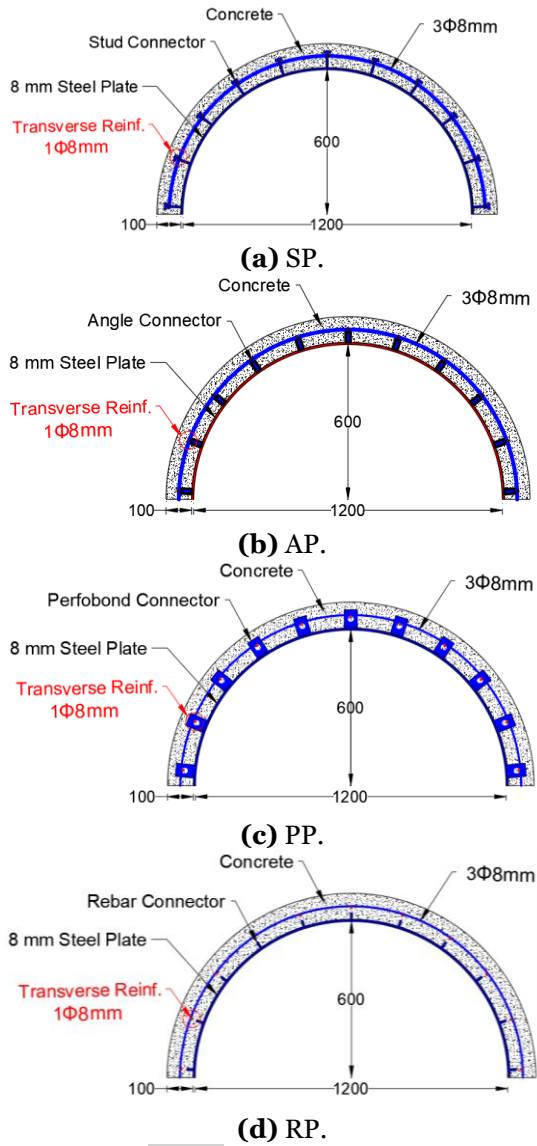


Fig. 8 SPCM Samples.

Eight steel molds were prepared and oiled properly. Then, the steel reinforcement was fixed in the right positions for casting samples, as shown in Fig. 9. All arch beam concrete parts were cast simultaneously with the same concrete proportion. The concrete was cured for the required period to be ready for the tests, as illustrated in Fig. 10. Figure 11 shows the testing rig details. The load cell is located under the 100-ton hydraulic jack of the load cell. LVDT is connected to data logger TDS-530 to record the load and deflection simultaneously along the tests' period for each 1 second. Precisions for load cell and LVDT were 0.01 kN and 0.01 mm, respectively. Four samples of the push-out test were cast. Each sample represents one type of the four connectors. The concrete part was reinforced using 4F8 mm longitudinal steel bars fixed with 3F8 stirrups. The details and dimensions of the push-out sample can be seen in Fig. 12. The casting process samples and testing is illustrated in Figs. 13 and 14.



Fig. 9 Arch Beams Steel Molds and Reinforcement.



Fig. 10 Casting and Curing of the Samples.

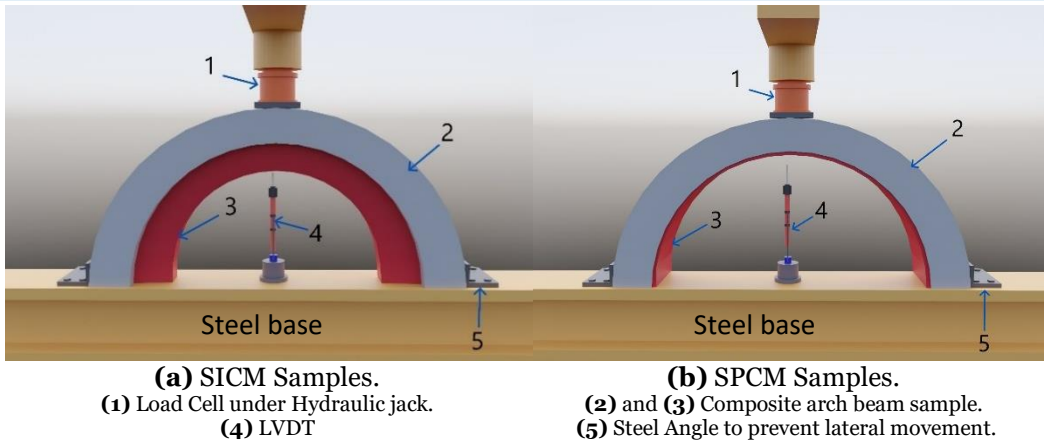


Fig. 11 Testing Rig Details.

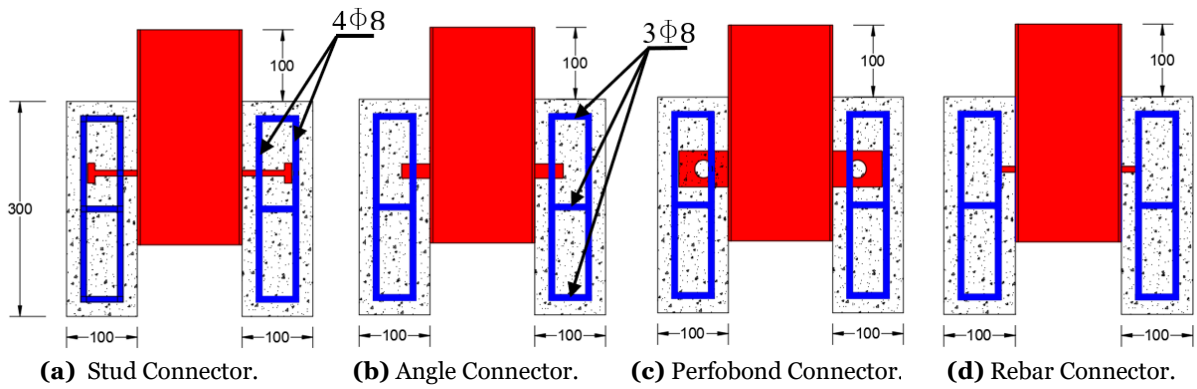


Fig. 12 Details and Dimensions of the Push-Out Samples.



Fig. 13 Push-Out Sample Casting Process.



Fig. 14 Push-Out Test.

4.RESULTS AND DISCUSSION

The tests were executed in two groups. The first group consisted of four samples of SICM using the four types of connectors. The SPCM was used for the second group using the same four types of connectors. [Figure 15](#) shows the samples under test.



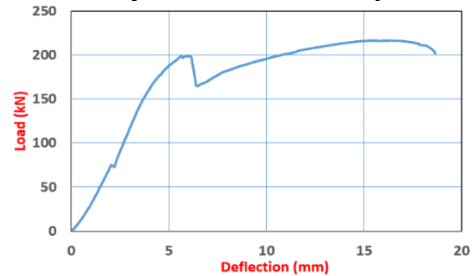
(a) SICM. **(b)** SPCM.

Fig. 15 Samples under Tests.

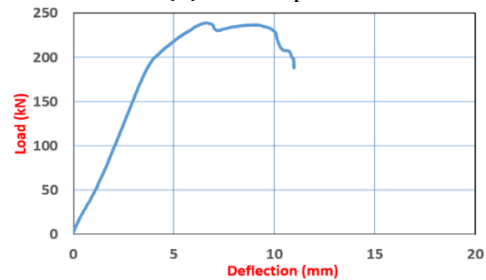
4.1.First Crack Load, Ultimate Load, and Deflection

[Figure 16](#) shows the load-deflection curves for SICM with different types of connectors. All the samples showed the same behavior; the only difference recorded at the SI sample curve was the drop of load at 200 kN load. [Table 7](#) shows the first crack, ultimate load, and deflection at ultimate load. As a comparison in this table, the SI sample is considered a reference. The differences in first cracks were 75% for AI, 67% for PI, and 108% for RI compared with the SI sample, respectively. The ultimate load for all samples in this group was relatively close. The maximum difference was 14.2% recorded for PI, while the minimum was 0.4% for the RI sample. A big variance can be noted when looking at the deflection at the ultimate load, where the maximum difference was -57% for the AI sample. [Figure 17](#) shows the load-deflection curves of all group samples. The AI

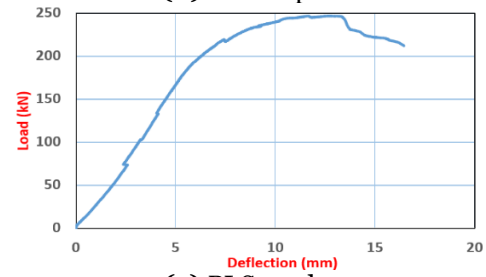
sample behaved stiffer, while the PI and SI had more flexibility than the other samples.



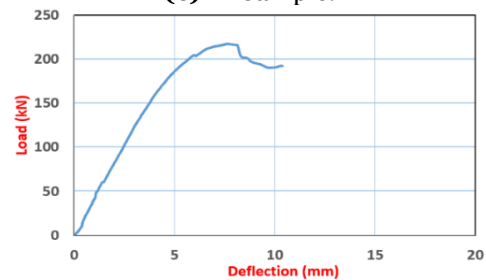
(a) SI Sample.



(b) AI Sample.



(c) PI Sample.



(d) RI Sample.

Fig. 16 Load Deflection Curves for SICM with Different Types of Connectors.

Table 7 SICM First Crack, Ultimate Load, and Deflection.

Sample Code	First Crack (kN)	%Diff. of First Crack	Ultimate Load (kN)	%Diff. of Ultimate Load	Deflection at Ultimate Load (mm)	%Diff. of Deflection at Ultimate Load
SI	60	0%	216	0%	15.5	0%
AI	105	75%	238.6	10.5%	6.6	-57%
PI	100	67%	246.6	14.2%	12.6	-18.7%
RI	115	108%	216.9	0.4%	7.6	-50.8%

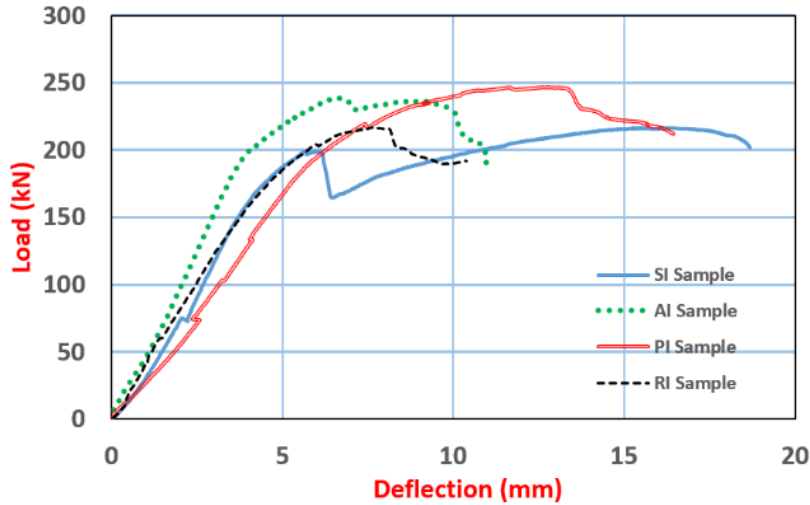
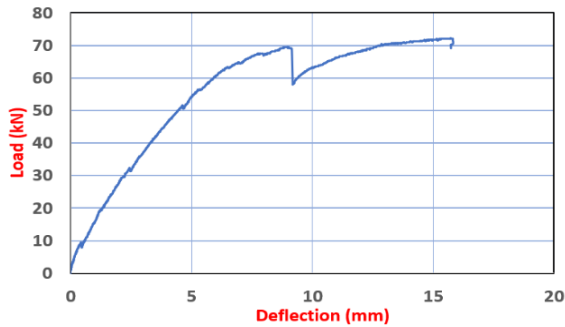


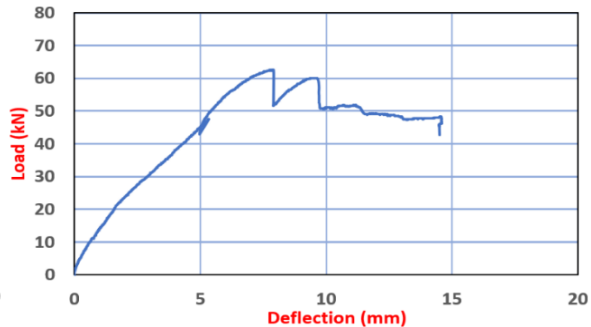
Fig. 17 Load-Deflection Curve for SICM Samples.

Figure 18 shows the load-deflection curves for the second SPCM group. All the samples showed the same behavior. The load drop for all samples can be seen at a given load value. Table 8 shows the first crack, ultimate load, and deflection at ultimate load; for the comparison in this table, the SP sample is considered a reference. The differences in first cracks were -16.3% for AP and 4.6% for PP with the SP sample, while SP and RP showed relatively the same amount. The highest ultimate load was

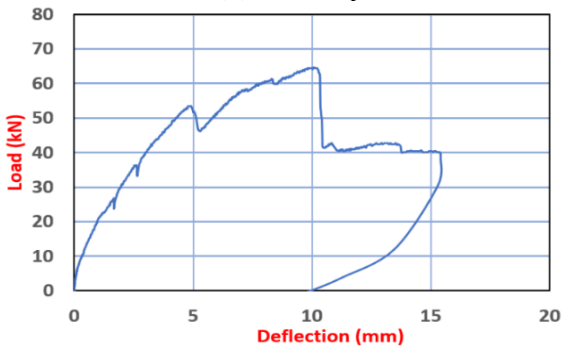
introduced by the SP sample, whereas the minimum was for the RP sample, which was 32% less than the SP sample. The deflection at the ultimate load for AP, PP, and RP samples was approximately close to each other, while high deference can be found for the SP sample, i.e., 15.7 mm. Figure 19 shows the load-deflection curves of all SPCM samples. The highest variance can be found in the RP sample, which had the lowest stiffness and ultimate load value.



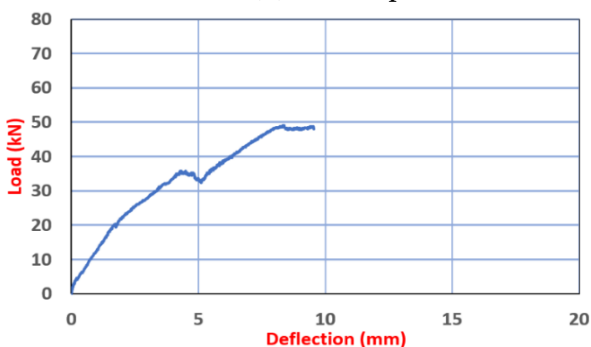
(a) SP Sample.



(b) AP Sample.



(c) PP Sample.



(d) RP Sample.

Fig. 18 Load Deflection Curve SPCM Using Different Types of Shear Connectors.

Table 8 SPCM First Crack, Ultimate Load, and Deflection.

Sample Code	First Crack (kN)	%Diff. of First Crack	Ultimate Load (kN)	%Diff. of Ultimate Load	Deflection at Ultimate Load (mm)	%Diff. of Deflection at Ultimate Load
SP	23.9	0%	72.3	0%	15.7	0%
AP	20	-16.3%	62.6	-13.4%	7.7	-51%
PP	25	4.6%	64.6	-10.7%	10	-36.3%
RP	24	0.4%	49.1	-32.1%	8.3	-47.1%

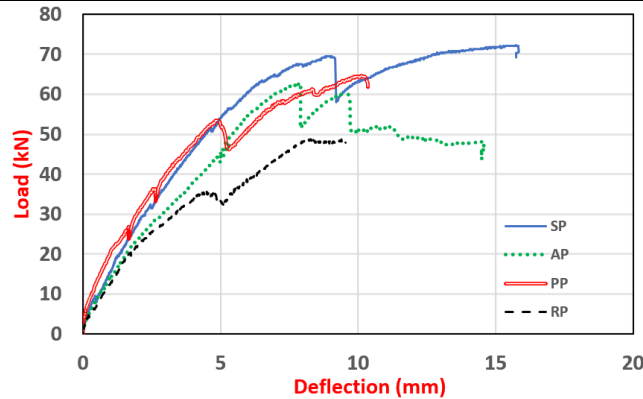
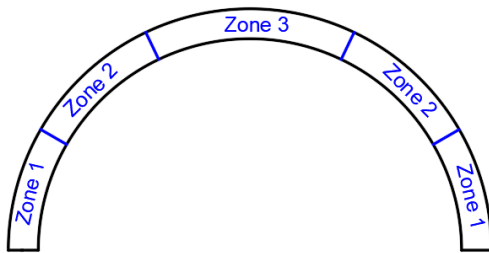


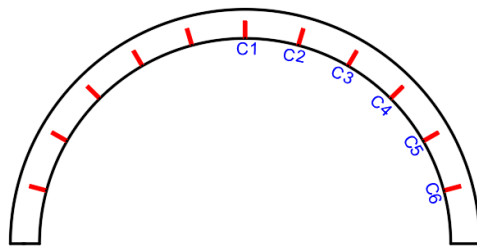
Fig. 19 Load Deflection Curve for SPCM Samples.

4.2. Effect of Shear Connectors on the Mode of Failure

For discussion reasons, the arch beam can be divided into three zones, as shown in Fig. 20 (a), and the connectors can be numbered, as shown in Fig. 20 (b).



(a) Beam Zoning.



(b) Connector Numbering.

Fig. 20 Arch Beam Notation.

Figure 21 illustrates the four SICM sample crack patterns. The first crack appeared at the outer surface of the concrete at zone 2 (-ve moment region) in all samples in this group. Then, the cracks generated gradually in Zone 3 and continued appearing in Zone 1. Finally, the failure crack appeared at the top of the beam, making an angle of nearly 30 degrees with the horizontal. In the SI sample, the concrete slipped upward at Zone 2 at one side of the beam, causing failure in the connector at this zone, which can be explained by the load drop in the load-deflection curve. The crack failure in this sample appeared in the vertical position.



(a) SI Sample.



(b) AI Sample.



(c) PI Sample.



(d) RI Sample.

Fig. 21 SICM Samples Crack Pattern.

Figure 22 illustrates the four samples for the SPCM crack patterns. The same behavior of the SICM group mentioned above can be found here. The failure shear crack at all samples appeared at the top of the concrete in the beam crown and extended to the bottom ward, making an angle between 30 and 45 degrees.



(a) SP Sample.



(b) AP Sample



(c) PP Sample.



(d) RP Sample.

Fig. 22 SPCM Samples Crack Patterns.

To identify the reason for the failure, the connectors were exposed by removing half of the concrete samples. The cause is the same for all samples; however, it is more obviously seen in sample PP. It was discovered that connector C2, through which the failure crack traveled, suffered from tension due to the considerable deflection under the load, mostly resulting in a vertical slip of the concrete from connector C2's top, as depicted in Fig. 23. A failure crack was also discovered to cut through the transverse bar reinforcement close to this connector. This concrete splitting explains the drops that happen at the load-deflection curves for SPCM

samples, accompanied by the crack appearance at these values of loads.



Fig. 23 High Vertical Slip in Connector C2.

The primary cause of failure may be the significant deflection under the load that produced tension at the C2 connector and resulted in the excessive vertical slip-off. Therefore, the connector used in steel-concrete composite arch members should be designed to carry more tension force than the shear force. Also, it is important to take care of the position and the magnitude of the transverse reinforcement bar to maintain the vertical slipping resistance in the concrete.

4.3. Shear Connector Resistance by Push-Out Test

Figure 24 shows the load-relative displacement for all samples in the push-out test. These figures show big differences in behavior and the ultimate load values. The perfbond connector introduced low stiffness at the beginning and the highest ultimate load and deflection. The ultimate load for the stud, angle, perfbond, and rebar connector was 69.3, 60.8, 101.5, and 90.7 kN, respectively.

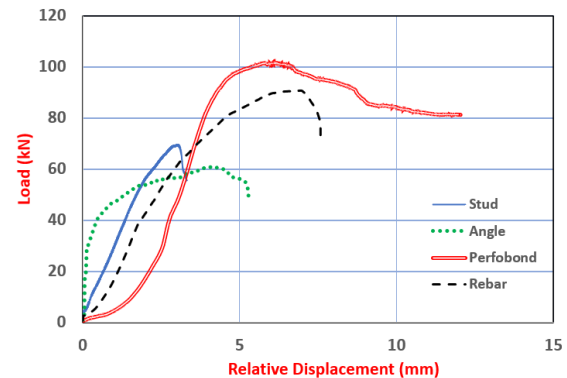


Fig. 24 Push out Load Relative Displacement Curve Using Different Types of Connectors.

5. CONCLUSIONS

The general conclusions can be drawn as follows:

- 1) The SICM introduced a higher ultimate load for all samples than the SPCM samples.
- 2) The SPCM was easier to implement and can be utilized for constructing low-load arch members at the lowest cost.
- 3) The failure shear crack in all samples appeared at the top of the concrete in the arch beam crown and extended to the

bottom, making an angle between 30 and 45 degrees.

- 4) The main reason for failure could be the considerable deflection under the load, which creates tension at the C2 connector (near the top arch beam connector) and causes a high vertical slip.
- 5) The connector used in steel-concrete composite arch members should be designed to carry more tension force than the shear force.
- 6) To maintain the vertical slipping resistance of the concrete, it is important to control the position and magnitude of the transverse reinforcement bar.

Also, the effect of the shear connector type can be summarized as follows:

- 1) The SICM samples showed the following results:
 - The maximum load causing the first crack was recorded at the RI sample and the minimum at the SI sample.
 - The ultimate loads for all samples were close to each other; however, the PI samples recorded the maximum ultimate of 14.2% compared to the SI sample.
 - The big variance was recorded for the sample's deflection at the ultimate, and the maximum was introduced by the RI sample.
- 2) The SPCM samples showed the following results:
 - The minimum load causing the first crack was recorded for the AP sample and the maximum for the PP sample.
 - The SP samples recorded the maximum ultimate load and deflections, while the minimum ultimate load was for the RP samples.
- 3) The longer connector can introduce better performance, as represented in the studied stud and perfobond connectors.

REFERENCES

- [1] Lacki P, Nawrot J, Derlatka A, Winowiecka J. **Numerical and Experimental Tests of Steel-Concrete Composite Beam with the Connector Made of Top-Hat Profile.** *Composite Structures* 2019; **211**: 244–253.
- [2] Chiorean CG, Buru SM. **Practical Nonlinear Inelastic Analysis Method of Composite Steel-Concrete Beams with Partial Composite Action.** *Engineering Structures* 2017; **134**: 74–106.
- [3] Lacki P, Nawrot J, Derlatka A. **Numerical Analysis of Segment of Steel-Concrete Bridge Girder Loaded by Dead Load.** *Zeszyty Naukowe Politechniki Częstochowskiej seria Budownictwo* 2019; **22**(1): 204-212.
- [4] Zanzari AS, Yerudkar DS, Sharma MR. **Fire Behaviour of Composite Structure.** *International Journal of Engineering Research & Technology* 2021; **10**(8): 25-29.
- [5] Aziz IA, Mohammed KI. **State-of-the-art for Strengthening and Rehabilitating Structural Beams Using Carbon Fiber Reinforced Polymers Configurations (A Review).** *Al-Rafidain Engineering Journal* 2022; **27**(2): 49–59.
- [6] Bedewi A, Yahia YIO, Abdulla AI. **Reinforced Concrete Structures in Structural Behavior of Hollow Beam Reinforced with Different Types of GFRP Stirrups: Structural Behavior of Hollow Beam Reinforced with Different Types of GFRP Stirrups.** *Tikrit Journal of Engineering Sciences* 2023; **30**(1): 72–83.
- [7] Khalid AA, Abdulla FA, Al-Sharify M. **Experimental Investigation on the Fatigue Behavior on Honeycomb Sandwich Composite Panels.** *Tikrit Journal of Engineering Sciences* 2023; **30**(2): 122–129.
- [8] Alsultani AS, Najla'a H. **Flexural Behavior of Rectangular Double Hollow Flange Cold-Formed Steel I-Beam.** *Tikrit Journal of Engineering Sciences* 2023; **30**(4): 28–35.
- [9] McCormac JC, Csernak SF. **Structural Steel Design.** New York: Pearson, 2018.
- [10] Al-Darzi SYK, Al-Juboory LIMA. **Investigation of Steel-Concrete Composite Beams with Different Types of Shear Connectors.** *Tikrit Journal of Engineering Sciences* 2013; **20**(3): 32–40.
- [11] Johnson RP. **Composite Structures of Steel and Concrete: Beams, Slabs, Columns and Frames for Buildings.** John Wiley & Sons, 2018.
- [12] Kurrer KE, Kahlow A. **Arch and Vault from 1800 to 1864.** *Arch Bridges.* CRC Press, 2020: 37–42.
- [13] Proske D, Van Gelder P. **Safety of Historical Stone Arch Bridges.** 1st ed., Heidelberg: Springer Science & Business Media; 2009.
- [14] Hamza BH. **Behavior of RC Curved Beams with Openings and Strengthened by CFRP Laminates.** Ph.D.Thesis. University of Basra; Basra, Iraq; 2013.
- [15] Oliveira DV, Lourenço PB, Lemos C. **Geometric Issues and Ultimate Load Capacity of Masonry Arch Bridges from the Northwest Iberian Peninsula.** *Engineering Structures* 2010; **32**(12): 3955–3965.
- [16] Zhan Y, Duan M, Zhang L, Liu C, Li Z,

- Zhao R. **Study on the Shear Performance of Adhesive Shear Connectors in Push-Out Tests.** *Structures* 2021; **32**: 2103–2117.
- [17] Souici A, Berthet JF, Li A, Rahal N. **Behaviour of Both Mechanically Connected and Bonded Steel–Concrete Composite Beams.** *Engineering Structures* 2013; **49**: 11–23.
- [18] Fan L, Zhou Z. **New Shear Connectors Based on PBL Shear Connector for Composite Arch Members.** *Structural Engineering International* 2014; **24**(2): 281–284.
- [19] Ali YA, Kadhum MJ. **Nonlinear Analysis for behavior of Hollow Box Reinforced Concrete Arch Beams with Transverse Openings.** *Nonlinear Analysis* 2015; **7**(11): 66–74.
- [20] Mansur MA. **Design of Reinforced Concrete Beams with Web Openings.** *Proceedings of the 6th Asia-Pacific Structural Engineering and Construction Conference (ASPEC 2006)*. Citeseer, 2006; Malaysia: Kuala Lumpur: p. 5–6.
- [21] Zhou Z, Fan L, Wang S, Liao X. **Chongqing Wansheng Zaodu Bridge – Steel Box–Concrete Composite Arch Bridge.** *Structural Engineering International* 2013; **23**(1): 71–74.
- [22] Ali AY, Hamza BA. **Finite Element Analysis of RC Arches with Openings Strengthened by CFRP Laminates.** *COMPLAS XIII: Proceedings of the XIII International Conference on Computational Plasticity: Fundamentals and Applications* 2015; Barcelona, CIMNE: 495–506.
- [23] Jayanthi V, Umarani C. **Performance Evaluation of Different Types of Shear Connectors in Steel-Concrete Composite Construction.** *Archives of Civil Engineering* 2018; **64**(2): 97–110.
- [24] Ibrahim AM, Salman WD, Bahlol FM. **Flexural Behavior of Concrete Composite Beams with New Steel Tube Section and Different Shear Connectors.** *Tikrit Journal of Engineering Sciences* 2019; **26**(1): 51–61.
- [25] Lu P, Zhang J, Li D, Zhou Y, Shi Q. **Conceptual Design and Experimental Verification Study of a Special-Shaped Composite Arch Bridge.** *Structures* 2021; **29**: 1380–1389.
- [26] Nimnim HT, Fakhri AH. **Structural Behavior of High Strength Arched Reinforced Concrete Slabs.** *Kufa Journal of Engineering* 2022; **13**(2): 1-15.
- [27] Iraqi Standard I.Q.S. **The Aggregate of The Natural Sources Used in Concrete, No. 45.,** 2010.
- [28] American Society of Testing and Materials (ASTM), **Standard Test Method for Relative Density (Specific Gravity) and Absorption of Fine Aggregate.** ASTM C128-15, West Conshohocken, PA, USA, .
- [29] American Society of Testing and Materials (ASTM), **Standard Test Method for Relative Density (Specific Gravity) and Absorption of Coarse Aggregate.** ASTM C127-15, West Conshohocken, PA, USA.
- [30] American Society of Testing and Materials (ASTM), **Standard Test Method for Sieve Analysis of Fine and Coarse Aggregates.** ASTM C136-06, West Conshohocken, PA, USA.
- [31] American Society of Testing and Materials (ASTM), **Standard Specification for Deformed and Plain Carbon-Steel Bars for Concrete Reinforcement.** ASTM A615/A615M-20, West Conshohocken (2020).
- [32] ACI 211.1-91. **Standard Practice for Selecting Proportions for Normal, Heavyweight, and Mass Concrete.** ACI Manual of Concrete Practice, Part 1: Materials and General Properties of Concrete, Detroit, Michigan, 1994.
- [33] American Society of Testing and Materials (ASTM). **Standard Test Method for Slump of Hydraulic-Cement Concrete.** ASTM C143/C143M-12, West Conshohocken, PA, USA.
- [34] American Society of Testing and Materials (ASTM), **Standard Test Method for Compressive Strength of Cylindrical Concrete Specimens.** ASTM C39/C39M-21,, West Conshohocken (2021).
- [35] American Society of Testing and Materials (ASTM), **ASTM A36/A36M-19, Standard Specification for Carbon Structural Steel.** ASTMA36/A36M-19, West Conshohocken, PA, USA, 2019.